Journal of Neurocytology **29**, 227–239, 2000

Hair cells in the inner ear of the pirouette and shaker 2 mutant mice

LISA A. BEYER[1], HANA ODEH[1], FRANK J. PROBST[2], ERICA H. LAMBERT[1], DAVID F. DOLAN[1], SALLY A. CAMPER[2], DAVID C. KOHRMAN[1] and YEHOASH RAPHAEL[1]*

[1] *The Department of Otolaryngology, Kresge Hearing Research Institute, School of Medicine, The University of Michigan, USA*

[2] *The Department of Human Genetics, School of Medicine, The University of Michigan, USA*

Received 16 February 2000; revised 7 April 2000; accepted 15 May 2000

Summary

The shaker 2 (*sh2*) and pirouette (*pi*) mouse mutants display severe inner ear dysfunction that involves both auditory and vestibular manifestation. Pathology of the stereocilia of hair cells has been found in both mutants. This study was designed to further our knowledge of the pathological characteristics of the inner ear sensory epithelia in both the *sh2* and *pi* strains. Measurements of auditory brainstem responses indicated that both mutants were profoundly deaf. The morphological assays were specifically designed to characterize a pathological actin bundle that is found in both the inner hair cells and the vestibular hair cells in all five vestibular organs in these two mutants. Using light microscope analysis of phalloidin-stained specimens, these actin bundles could first be detected on postnatal day 3. As the cochleae matured, each inner hair cell and type I vestibular hair cell contained a bundle that spans from the region of the cuticular plate to the basal end of the cell, then extends along with cytoplasm and membrane, towards the basement membrane. Abnormal contact with the basement membrane was found in vestibular hair cells. Based on the shape of the cellular extension and the actin bundle that supports it, we propose to name these extensions "cytocauds.'' The data suggest that the cytocauds in type I vestibular hair cells and inner hair cells are associated with a failure to differentiate and detach from the basement membrane.

Introduction

Hereditary inner ear disease in mice often results in functional and structural deficits in the auditory and vestibular portions of the inner ear (Steel & Brown, 1996). This makes the mouse a useful model for studying genetic inner ear disease. Mutations in any one of a large number of genes are also involved in human hereditary disease. The ultimate goal of studies of mice with hereditary inner ear disease is to identify and characterize the associated genes and develop therapeutic measures such as gene therapy.

Depending on the function of the mutated gene, pathological changes can be observed in a variety of cell types in the inner ear. Pathologies in hair cells have been characterized in several mouse mutants, such as Snell's waltzer (Avraham *et al*., 1997), shaker 1 (Hasson *et al*., 1997) and shaker 2 (*sh2*) (Probst *et al*., 1998). It is not always clear if a pathological characteristic found in a certain cell type is the primary result of the mutation or a secondary response to it. Therefore, detailed studies of the earliest pathological manifestations of each mutation are needed to identify the affected cells and determine their disrupted cellular function.

The normal structure of hair cells is well characterized (Slepecky, 1996). Because of the high order seen in the dimension and organization of these cells, any deviation can be readily detected. Notably, changes in shape, number, size and the organization of the stereocilia have been observed and carefully characterized in a variety of mutants (Steel, 1995). The resolution and three-dimensional representation obtained by using scanning electron microscopy has greatly enhanced this type of analysis. Intracellular changes at the ultrastructural (transmission electron microscope) level have also been described (Bock & Steel, 1983; Steel & Bock, 1983). Typical findings include varying degrees of degenerative changes in the sensory and nonsensory regions of the inner ear. Perhaps one of the most unusual pathologies reported in hereditary inner ear disease is the long and cylindrical organelles that are unique to certain mutants.

* To whom correspondence should be addressed.

0300–4864

These cylindrical organelles were first described by Ernstson *et al*., (1969) in the vestibular hair cells of waltzing guinea pigs, and were further characterized by Sobin and Flock (1981). Transmission electron microscopy has revealed that these structures are oriented along the apical-basal axis of the hair cells, spanning from the cuticular plate at the apical end to the plasma membrane at the basal end of the cell. In some cases, the organelles were described to push against the plasma membrane at the basal end of the cell, forming a bulge. These organelles were subsequently shown to contain actin (Sobin & Flock, 1983), and were named actin rods due to their shape and molecular contents (Sobin *et al*., 1982; Sobin & Flock, 1983).

Innovative improvements in imaging technology and in tools for molecular analysis have significantly enhanced our ability to assess the morphological manifestations associated with mutations. As a result, several genes that are responsible for hereditary inner ear diseases have been identified in both humans and mice. The main purpose of the experiments reported here was to analyze the pathology of the auditory and vestibular epithelium in *sh2* and pirouette (*pi*) mice, especially the morphological features of their actin-rich cellular projections. We found an abnormal cell shape in the inner hair cells and in the vestibular epithelium of type I hair cells in these mutants. In each of these types of cells, the pathology includes a narrow, tail-like extension of the cell body towards the basement membrane. The core of the extension is a long, cylindrical and highly organized bundle of actin filaments. Due to the lengthy tail-like appearance, we have named the extension in each of these hair cells a "cytocaud". Cytocauds extend basally for a distance more than double the length of the hair cell to reach the basement membrane or its vicinity.

Materials and methods

ANIMALS AND GENOTYPE ANALYSIS

We report experiments performed on two strains of mice with inner ear defects, *sh2* and *pi*, which exhibit the recessively inherited traits of hearing loss and vestibular dysfunction. Animal care and handling were approved by the University of Michigan Institutional Committee on the Use and Care of Animals and were performed using accepted veterinary standards.

Homozygous and heterozygous *sh2* mutants ages 12 and 16 days were used. The *sh2* mutation was maintained on a mixed genetic background. At least four animals of each age were used for each group. Affected mice that displayed circling, abnormal head movement, abnormal righting response and absence of Preyer's reflex were inferred as *sh2* homozygotes.

Postnatal homozygote and heterozygote *pi* mice were examined at the ages of 2, 3, 5, 12, 16, 21 and 30 days. These mice were originally obtained from the Jackson Laboratory (Bar Harbor, ME). The *pi* mutation, since arising on a C3H mouse strain, has been maintained by repeated backcross matings to strain C57BL/6J. After greater than 18 backcross generations, the mutation is congenic on the C57BL/6J background, within a C3H-derived interval of less than 6 cM in size (DCK, unpublished). Each group included at least four animals. In animals 12 days and older, observation of the phenotype could be used to determine the genotype. The allelic status of younger mice was determined by genotype analysis of genomic DNA. *D5Mit197* and *D5Mit355* are simple sequence length polymorphism markers (SSLP) located proximally and distally, respectively, of the *pi* locus, within the C3H congenic region (DCK, unpublished). Both markers exhibit allelic size differences between the C57BL/6J and C3H strains of greater than 14 bp (primer sequences, PCR conditions, and strain allele sizes are available at the Whitehead Institute for Biomedical Research/MIT Center for Genome Research).

Genomic DNA was prepared from the offspring of C57BL/6J-pi/pi X C57BL/6J-*pi*/+ matings by incubation of toe biopsies at 60° C for 2 h. in DNA extraction buffer (50 mM KCl; 10 mM Tris-Cl pH 8.3; 1.5 mM $MgCl_2$; 0.45% (vol/vol) NP-40; 0.45% (vol/vol) Tween 20), followed by boiling for 10 min. DNA was amplified by PCR under standard conditions with SSLP primer sets specific for *D5Mit197* and *D5Mit355*. Amplification products were separated by electrophoresis on 3% agarose gels and visualized by ethidium bromide fluorescence. Control *pi*/+ pups were identified as those that were heterozygous for the C57BL/6J and C3H alleles at both markers. Homozygous *pi*/*pi* pups were identified as those that exhibited only the C3H alleles at both markers.

AUDITORY BRAINSTEM RESPONSES (ABRs)

Animals were anesthetized with a mixture of xylazine (0.00125 mg/kg for animals <8.0 g and 0.004 mg/kg for mice >8 g) and ketamine (0.0625 mg/kg for animals <8 g and 0.12 mg/kg for mice >8 g) prior to measurement. The animals were placed in a sound-isolated, electrically-shielded booth (Acoustic Systems) on a heating pad. Needle electrodes (Grass E2 platinum) were placed subcutaneously below the tested ear (reference electrode), and in the vertex (active electrode). The ground electrode was inserted below the contralateral ear. The sound stimulus consisted of 15 ms tone bursts, (rise-fall time 1 ms) at 1, 8 and 24 kHz. The sound stimuli were delivered into the ear canal from an encased, shielded Beyer earphone through a tube (13 mm). Response waveforms (100,000 gain, filtered from 0.3–3.0 kHz) were averaged (1,024 epochs) using a Tucker-Davis data acquisition system. The response threshold was defined as the interpolated value between the last level in which a response was present and 5 dB lower where no response was observed.

MORPHOLOGY

Three types of morphological analyses were performed: scanning electron microscopy (SEM), transmission electron microscopy (TEM) and whole mount analysis of phalloidin-stained samples. SEM was used to identify the characteristics of the surface features associated with the intracellular presence of a cytocaud. TEM was performed to identify the ultrastructural features of cytocauds, their association with other organelles, and their sites of initiation and termination.

Phalloidin epifluorescent analysis was used to determine the tissue distribution of the cytocauds, the degree of uniformity between the cells that exhibit cytocauds, the number of cytocauds per cell and the typical longitudinal dimensions of the cytocauds.

For TEM analysis, the animals were anesthetized and fixed by intracardiac perfusion with 2.5% glutaraldehyde in 0.15 M cacodylate buffer. The inner ear was removed and immersed in fixative for 2 h. The cochlea and vestibular tissues (utricles, saccules and ampullae) were dissected and decalcified for 1 week in 3% EDTA with 0.25% glutaraldehyde. The tissue was stained en bloc in 0.1% uranyl acetate for 30 min. and then post-fixed with 1% osmium tetroxide in phosphate buffer for 1 h. The specimens were dehydrated in increasing ethanol concentrations and embedded in Embed 812 epoxy resin. Sections were taken on a Leica Ultracut R using a diamond knife, stained with uranyl acetate and lead citrate, and examined on a Philips CM-100 TEM.

For SEM analysis, the animals were anesthetized and systemically perfused with fixative as described above. The cochleae were processed using the OTOTO method (Osborne *et al*., 1991) or traditional SEM preparation, as previously described (Raphael *et al*., 1991). For the traditional preparation, tissues were post-fixed with 1% osmium tetroxide in phosphate buffer for 1 h., dehydrated through an ethanol series and critical point dried with CO_2 in a Samdri 790. Samples were mounted on stubs, sputter coated with gold (Polaron E5100) and examined with an Amray 1000B SEM. For OTOTO preparation, the tissues were immersed alternately in thyocarbohydrazide and osmium tetroxide. They were then critical point dried and mounted on stubs for analysis.

For phalloidin analysis, animals were anesthetized and the temporal bones removed. The temporal bones were immersed in 3% paraformaldehyde in phosphate buffer (0.15 M, pH 7.35). Under stereoscopic magnification, the round and oval windows were opened and the bone from the apical tip of the cochleae was removed to allow flow of fixative throughout the tissue. Two hours later, the otic capsule was trimmed to reveal the two cochlear turns. The entire apical turn and several fragments of the basal turn were separated from the modiolus and from the lateral wall tissues. Samples were permeabilized in Triton X-100 (0.3%, 5 min.) and incubated with rhodamine phalloidin (Molecular Probes, Eugene, OR) 1 : 100 in PBS for 30 min. After thorough rinsing, the tissues were mounted on glass slides with CrystalMount (Biomeda, Foster City, CA). Tissues were analyzed and photographed on a Leica DMRB epifluorescent microscope using ×10, ×40 oil and ×100 oil objectives and a standard TRITC filter. Photographs were taken using Kodak Ektachrome 320 film.

Confocal microscopy (CFM) was used to localize the cytocauds at a high resolution, and to determine their orientation and dimension (length and cross-section). Whole mounts of the apical cochlear turn and the utricle were prepared for phalloidin staining as described, then analyzed with a ×63 N/A 1.4 objective in a Nikon Diaphot microscope and a BioRad MRC-600 laser scanning microscope. Z-series (1 μm interval) were taken from the apical portion of the sensory epithelium, spanning the entire epithelial layer and terminating at the extracellular matrix beneath the epithelium. Files were converted and stored as TIFF files. The stack of Z-series was then converted to separate windows using NIH Image.

Results

ABRs

ABR thresholds of *pi/pi* mice at several developmental stages demonstrate their profound deafness (Fig. 1). No responses can be obtained from either the *pi* or C57BL/6J mice at 12 days (data not shown). At 14 days, as functional maturation of the auditory system is more advanced, the C57BL/6J mice exhibit hearing at all three frequencies tested. Thresholds progressively improve through day 24 (Fig. 1). The values at day 24 for the C57BL/6J mice are comparable to the values reported by others (Li & Borg, 1993). In contrast, during the same developmental period in the *pi* mice, response waveforms cannot be elicited at any frequency except for 8 kHz. At this frequency, thresholds are observed in response to stimuli of 90 dB SPL or higher, indicating a profound hearing loss. No ABR responses are observed at 1.0 and 24.0 kHz, at stimulus intensities ranging from 110–120 dB SPL. No ABR responses, at any stimulus frequency, are observed in *pi* mice after 30 days of age.

SEM

The surface morphology of the organ of Corti is found to be abnormal in both the *sh2* and *pi* mutants (Fig. 2). In the *sh2* mouse ears, inner hair cells at 21 days after birth display very short stereocilia, organized in supernumerary rows, which cover most of the apical surface of these cells (Fig. 2A). Tip links are not seen between the stereocilia of two adjacent rows. Kinocilia are absent. With the exception of the short stereocilia and a few microvilli, no other cellular extension into the lumen is observed. A normal-appearing population of supporting cells surround the hair cells. The shape and degree of differentiation of the supporting cells appear normal or close to normal.

In the mature (P30) *pi* organ of Corti, inner hair cell stereocilia appear short and disorganized (Fig. 2B). The number of the stereocilia on each cell appear smaller than normal. The typical two-row organization and height gradation is absent. Tip-links and kinocilia are not seen. No major abnormalities are evident on the surface of the supporting cells.

The inner hair cells in a wild-type control mouse (C57BL/6J) show the typical two-row organization, with one tall row and one shorter row (Fig. 2C). The stereocilia of the shorter row are connected to the taller ones with tip-links. Side-links are also present between the individual stereocilia of the taller row. Kinocilia are absent in normal mature auditory inner hair cells.

PHALLOIDIN HISTOCHEMISTRY IN THE ORGAN OF CORTI

Epifluorescence examination of phalloidin-stained whole mounts of the organ of Corti reveals the normal

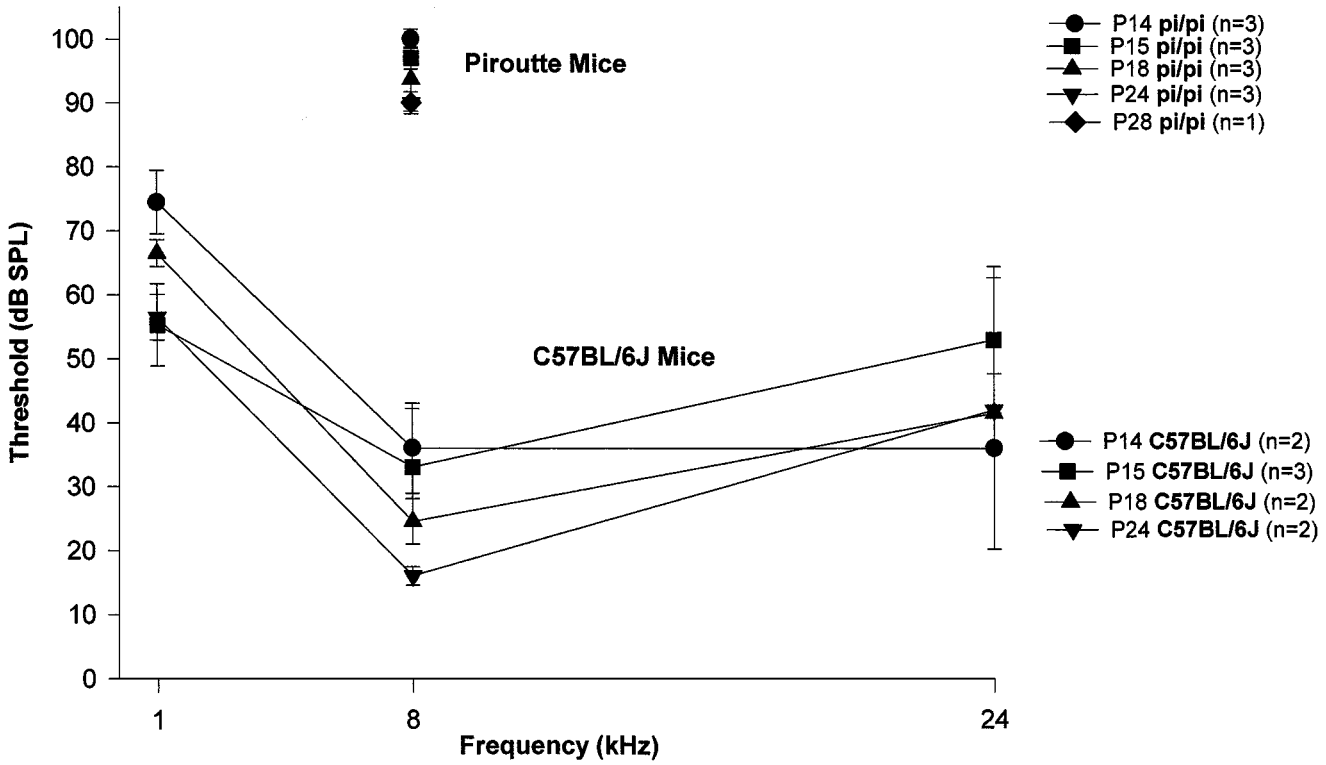

Fig. 1. ABR thresholds, as a function of age, are shown for the *pi/pi* and C57BL/6J mice. At the end of the first postnatal month, C57BL/6J mice show thresholds approaching adult values. Prior to 14 days after birth, no responses could be obtained from either strain at the acoustic limits of the delivery system. Responses were only obtained from the *pi/pi* mice at 8 kHz. After 28 days, no response was observed from the *pi/pi* mice at any frequency.

organization of this organ in 16-day old control mice. At a focal plane just above the reticular lamina (the luminal surface of the auditory epithelium), a normal organization of cells and a normal appearance of stereocilia are evident (Fig. 3A). The stereocilia of the inner hair cells are readily visible. At a lower focal plane just beneath the cuticular plate, an actin signal is seen in the cuticular plate of the inner hair cells (Fig. 3B). In a *sh2/sh2* animal of a similar age, the signal for the stereocilia and cuticular plate is very weak (not shown). However, just beneath the reticular lamina, a thick actin bundle is seen, extending from each inner hair cell in a medial course, towards the modiolar axis of the cochlea (Fig. 4). The general orientation of each bundle is similar to the others. In some of the bundles, one or more kinks are observed, but the general direction is medially oriented. The length of each bundle exceeds 30 μm. During analysis under epifluorescence, it is possible to follow the course of these actin bundles. The apical end of each bundle appears to be at or near the cuticular plate, just beneath the luminal surface of the inner hair cells. As the focus is lowered towards the basal domain of these cells, the actin bundles first extend directly down the Z axis, then turns sharply towards the medial axis of the cochlea. Once the bundles turn, they proceed medially in a plane that is parallel to the basement membrane (Fig. 4).

CFM images of the inner hair cell region in a 30-day old *pi/pi* mouse reveal optical sections at three different focal planes (Fig. 5). Compared with normal mice (Fig. 3A), the fluorescence in stereociliary bundles of the *pi/pi* stereocilia is very faint, suggesting a decreased amount of actin in the stereocilia and the cuticular plate. At the focal plane of the cuticular plate, every inner hair cell has an intense signal shaped as a circle (Fig. 5A). The bright circle is typically located close to the center

Fig. 2. SEM images of the surface of the mature inner hair cells in the lower apical turn of the organ of Corti of *sh2/sh2* (A) *pi/pi* (B) and control (C) mice. The top part of all three images is oriented in the lateral aspect of the organ of Corti (towards the outer hair cells). (A) In the *sh2/sh2* mouse ears, the inner hair cell stereocilia are short and their number is larger than normal. They form 5–6 rows. Tip links and kinocilia are not seen. (B) Inner hair cell stereocilia of a mature *pi/pi* organ of Corti appears short and disorganized. The number of the stereocilia on each cell appears smaller than normal. The typical two-row organization and height gradation is absent. Tip-links and kinocilia are not seen. (C) Inner hair cell stereocilia in a control mouse (C57BL/6J) are organized in two rows, one much taller than the other. Stereocilia of the two rows are inter-connected by tip-links (large arrow), whereas stereocilia of the same row are connected with side-links (small arrows). Bar is 2 μm for (A), (B) and (C).

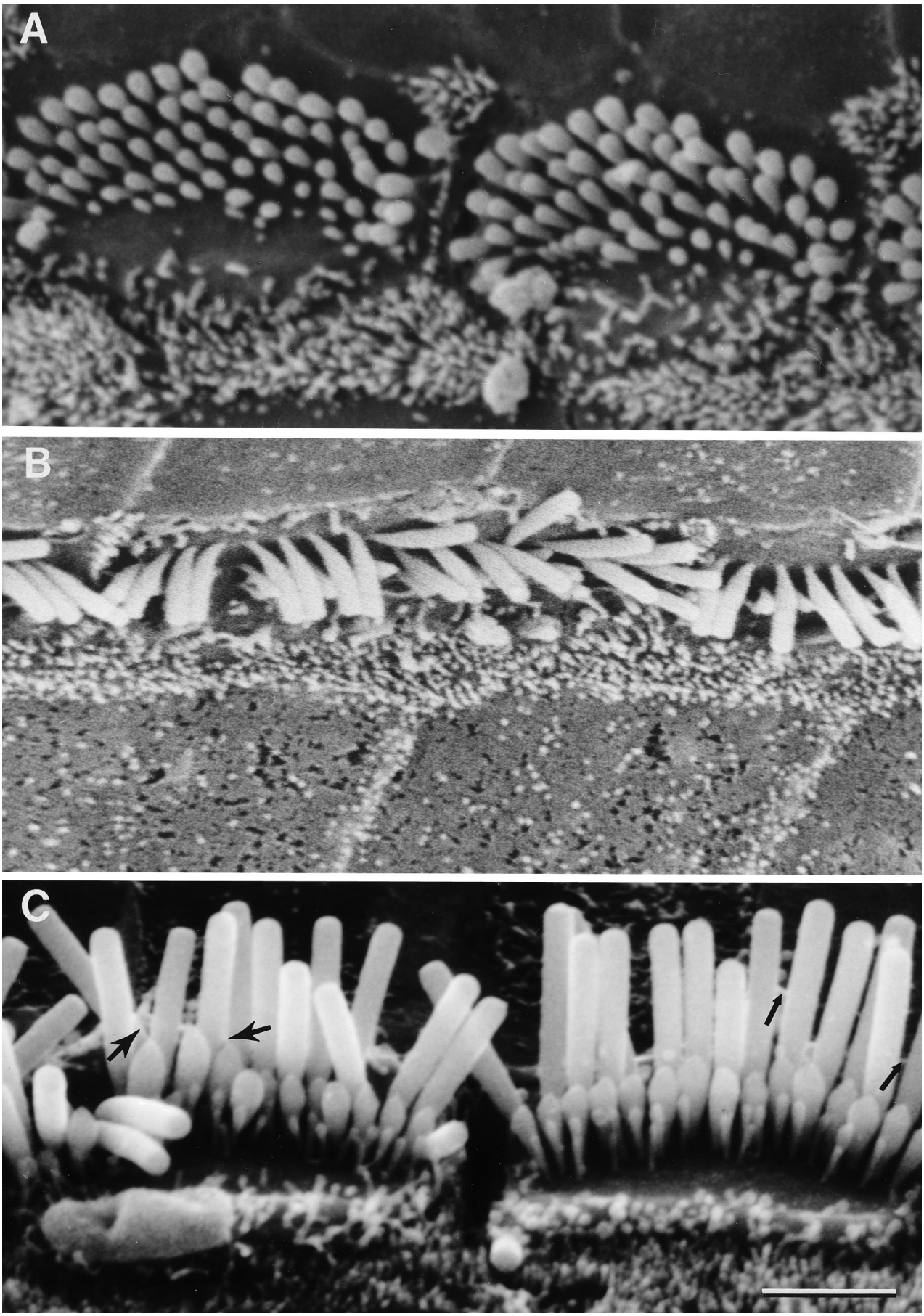
A
B
C

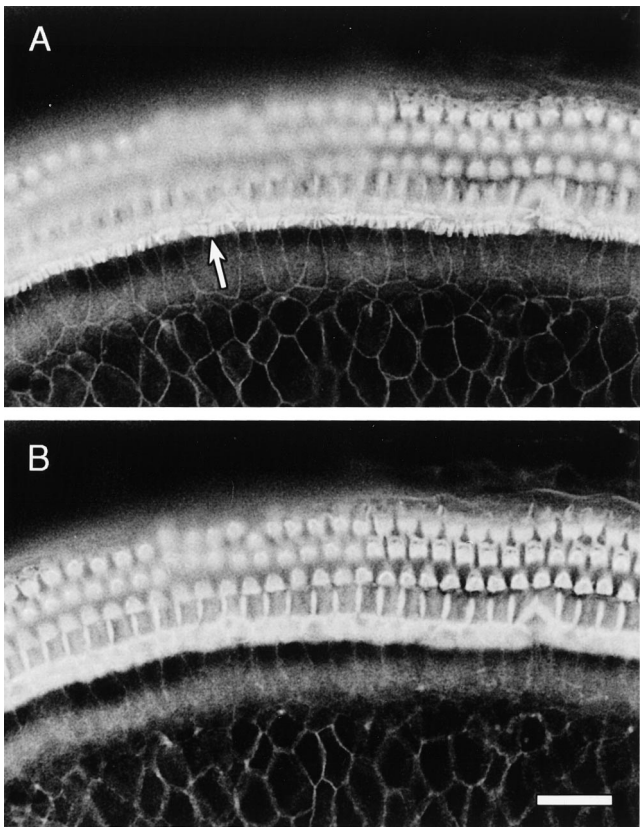

Fig. 3. Epifluorescent images of a whole mount of the organ of Corti of a 16-day old control (wild-type C57BL/6J) mouse labeled with phalloidin. (A) At a focal plane of the inner hair cell stereocilia, a full complement of hair cells with normal-length hair bundles is seen (arrow). (B) At a lower focal plane of the same visual field, actin-positive stain is detected in the cuticular plate of inner hair cells. Bar is 25 μm.

of the cell, but in some cases it is off-center, closer to the lateral membrane. All cells have at least one bright spot, but 3–4 inner hair cells in every cochlea have two spots (Fig. 5A). These bright circles represent (optical) cross sections through the actin core of the cytocauds at their apical domain, close to the cuticular plate. Below the cuticular plate (2 μm), approaching the level of the inner hair cell nuclei, the bright spots are still circular in shape (Fig. 5B).

At a more basal focal plane (Fig. 5C), each actin bundle changes direction and appears as a tail-like extension, protruding from each inner hair cell in a medial direction. In every inner hair cell, this actin core of the cytocaud extends medially (toward the modiolus) spanning a distance of 35–40 μm. Several kinks (1–3) are found in most of the cytocaud cores (Figs. 4 and 5C), but some are straight. Cytocauds found in the *sh2* cochleae are similar to those found in the *pi* mutant. In both the *sh2* and *pi* mice, the cochlear cytocauds are limited to the inner hair cells.

PHALLOIDIN HISTOCHEMISTRY OF THE VESTIBULAR EPITHELIUM

Throughout the crista of each ampulla of mature *pi/pi* mice, the actin cores of the cytocauds extend towards the basement membrane in a course that is perpendicular to the plane of the luminal surface. Due to the saddle-like shape of the crista ampullaris, it is possible to observe horizontally-oriented cytocauds extending from the hair cells that are located on the rolling sides of the sensory epithelium (Fig. 6). Vestibular cytocaud cores have fewer kinks than those in the cochlea and their straight appearance is striking especially in the crista ampullaris. Cytocauds in the vestibular epithelium of *sh2/sh2* mice appear similar to these observed in *pi* mice (data not shown). In the heterozygote animals ($pi/^{+}$), cytocauds are not found (data not shown).

CFM analysis of whole mount preparations of utricles stained with phalloidin reveal a population of hair cells that have faint actin-specific fluorescence in their cuticular plate and short stereocilia (Fig. 7A). In utricular hair cells, which are (optically) sectioned just beneath the cuticular plate, one bright circle is seen, positioned at or near the center of the cell (Fig. 7A). These bright spots are cross (optical) sections of vestibular cytocauds. At a lower focal plane, optical sections reveal no actin-specific signal other than the actin core of the cytocauds (Fig. 7B). As the focal plane is gradually lowered along the Z-series, it is possible to follow most of the bright spots over 35 μm (data not shown). Each bright spot can be followed (down the Z axis) with very little change in its horizontal plane (along the x-y axis). To the subjective eye, the diameter of the spots is rather uniform throughout different areas of the utricle.

THE DEVELOPMENT OF CYTOCAUDS

In order to identify the onset of cytocaud formation, the cochleae of younger *pi/pi* animals were analyzed with phalloidin epifluorescence. In 2-day old pups, cytocauds are not detected. In 3-day old mutant pups, the actin cores of cytocauds can be observed in inner hair cells in the lower base of the cochlea (Fig. 8), but not in the apical regions (not shown). The circular bright spot at the focal plane immediately beneath the reticular lamina (luminal surface) can be detected but its intensity is faint. No tail portion is detected at this stage. In 4-day old pups, the tail portion can be detected in the lower basal turn of the cochlea. At this time, bright spots are first detected near the luminal surface in the apical coil of the cochlea (data not shown). These observations suggest a base-to-apex gradient of cytocaud formation in the cochlea. By the end of the first week of postnatal development, cytocauds appear to reach a nearly mature size (not shown). Cochlear cytocauds are restricted to the inner hair cells at all developmental stages.

Fig. 4. An epifluorescent image of a whole mount of the organ of Corti of a 16-day-old *sh2/sh2* mutant mouse labeled with phalloidin. The focal plane is slightly beneath the luminal surface. Long actin-positive bundles extend from the region of the inner hair cells in a medial direction (towards the modiolus). One bundle is associated with each inner hair cell. One or more kinks are seen in some of the bundles, but the general medial direction is maintained. Bar is 50 μm.

TEM

Analysis of crista ampullaris (vestibular epithelium) of *sh2* and *pi* mutants show that the actin core of cytocauds originates at the cuticular plate of the hair cells (Fig. 9A). However, the actin bundle is not directly associated with the rootlets of the stereocilia, which appear to terminate independently of the cytocauds (not shown). The basal bodies are also found in an area that is away from the apical end of the cytocaud core. Along the course of the cytocaud, several areas of dense cross-filaments are observed (Fig. 9A). No clear periodicity is observed in the distance between the dense areas. As the actin cores of the cytocauds descend basally through the cytoplasmic domain, they often pass very close to the nucleus. Thus, the nucleus appears flattened against the cytocaud (Fig. 9B). TEM analysis enables the identification of the types of vestibular hair cell under observation, based on the calyx-type nerve terminals. All cells in which cytocauds are present can be identified as type I vestibular hair cells.

Cytocauds in the vestibular epithelium protrude from the basal end of the cell. This protrusion includes the plasma membrane, a bundle of actin filaments, a significant amount of cytoplasm and several mitochondria (Fig. 9C). Cytocauds in the utricle extend towards the basement membrane area immediately below the hair cell. The basal tip of the extension is in contact with the basement membrane (Fig. 9C). In some cases, the actin core of the cytocaud is split into two different bundles, which appear to re-unite at a lower region (Fig. 9D). The area enclosed between the two split bundles contains numerous microtubules.

At the area of contact between the basal tip of the cytocaud and the basal lamina, dense filaments appear to extend from the cell towards the extracellular matrix (Fig. 10A). In some cases, electron-dense finger-like protrusions are observed (Fig. 10B). Each of these dense protrusions is 300–400 nm long. In these areas, the membrane of the hair cell and the basement membrane are less distinct than normal. In cochlear inner hair cells, cytocauds have several kinks (Figs. 4 and 5C) and are therefore more difficult to follow over long distances with TEM sectioning.

Discussion

The principal findings are that (a) the cell body of vestibular type I hair cells in the *sh2* and the *pi* mutants extends towards the basement membrane and attach to it, and (b) auditory inner hair cells in these mice also

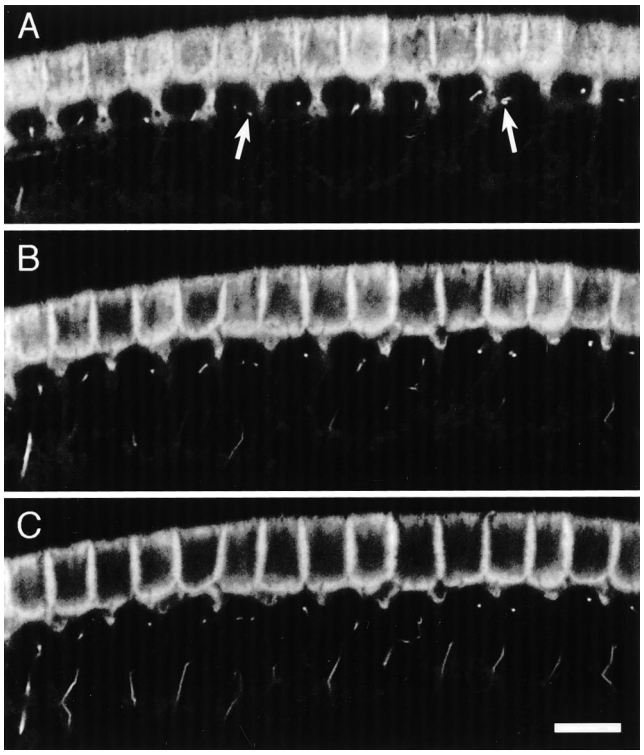

Fig. 5. Three sections from a Z-series of CFM optical sections through a phalloidin-labeled whole mount of a 30-day old *pi/pi* mouse. (A) At a focal plane of the cuticular plate of the inner hair cells, every inner hair cell has an intense actin-specific signal that is shaped as a circle or a short bar (arrows). One inner hair cell has two bright dots (left arrow). The bright circle is usually located close to the center of the cell, but in some cases it is off-center, closer to the lateral membrane. The actin-rich area at the top of the micrograph is the apical plate of the inner pillar cells. (B) At a focal plane 2 μm lower, toward the basal end of the cell, bright spots maintain their circular or bar-like appearance. In a more medial location, the tail-end domain of some of these actin bundles becomes visible. (C) At a focal plane close to the basal end of the inner hair cells, the actin bundles appear horizontal to the plane of the section, assuming the appearance of a tail-like extension protruding from each inner hair cell in a medial direction. In the actin bundle on the left-hand side, it is possible to observe the continuity between the dot in the inner hair cells and the tail-like portion that extends medially. The actin bundles have one or more kinks. Bar is 10 μm.

have extensions that protrude from the basal end of the cell and progress medially. Each extension contains a bundle of actin filaments, cytoplasm, mitochondria and other organelles. In naming these cellular extensions, we selected the term cytocaud, describing the tail-like appearance. The term cytocaud includes the actin core bundle along with the plasma membrane and cytoplasmic portion of the extension.

When describing a novel morphological feature of cells, it is important to verify that it is not an artifact. We have consistently observed a cytocaud in each and every inner hair cell in the *sh2/sh2* and *pi/pi* mice, but not in the normal control mice or in several different deaf mouse strains such as shaker 1, Ames waltzer, Snell's waltzer, spinner, deafness and mocha. Cytocauds have not been found in any outer hair cells. The consistency of the findings in inner hair cells and the absence of cytocauds in outer hair cells suggest that these structures are not preparation artifacts. This is supported by the fact that cytocauds can be detected by several different morphological methods: light microscopy (epifluorescent and CFM) of whole mounts with actin-specific stain and TEM.

The presence of an organelle with the appearance of an actin rod has been previously described in hair cells of the *sh2* mouse and the waltzing guinea pig (Ernstson *et al*., 1969; Anniko *et al*., 1980; Sobin & Flock, 1981; Sobin *et al*., 1982). In the waltzing guinea pig, actin rods were found in type I vestibular hair cells. In the *sh2* mouse, actin rods were found in the inner hair cells, in addition to the vestibular hair cells. These studies used sectioning techniques and were therefore unlikely to detect the entire extent of these organelles, and the connection to the basement membrane. They were named rods because only their straight domain, residing within the normal cell borders, was identified. This study confirms the original observation of actin rods, using a different method, the whole mount preparation. Using this preparation, we identified the entire length of these actin-rich organelles. Most importantly, we discovered that in vestibular hair cells, the cytocauds extend, along with a cytoplasmic projection, in a basal direction to make a connection with the basement membrane.

Using the phalloidin assay on developing inner ears, we detected cytocauds in *pi/pi* pups as early as 3 days postnatally. Within a given cell, it appears that the cytocauds grow from the apical domain towards the base of the cell. Comparing cytocaud assembly at different sites along the cochlear duct, it appears that the cytocauds follow the gradient that is usually found in cochlear differentiation, with earlier formation in the lower turn (high frequency region) than in the apical (upper) turn (Sher, 1971; Lim & Anniko, 1985). It is likely that cytocaud development begins before day 3, but it could not be detected by light microscope observation of phalloidin-labeled specimens. Further TEM analysis will be necessary to determine exactly when hair cells start to assemble these organelles.

While studying the actin rod, Sobin and Flock (1981) decorated the filament with myosin S1 subfragments and determined that the polarity of the actin bundle opposed that of the stereocilia. They suggested that the actin rods grow from the apical domain of the cell in a basal direction, with actin monomers added at the basal (plus) end. This finding is consistent with our developmental sequence, which shows that the cytocaud elongates basally during development.

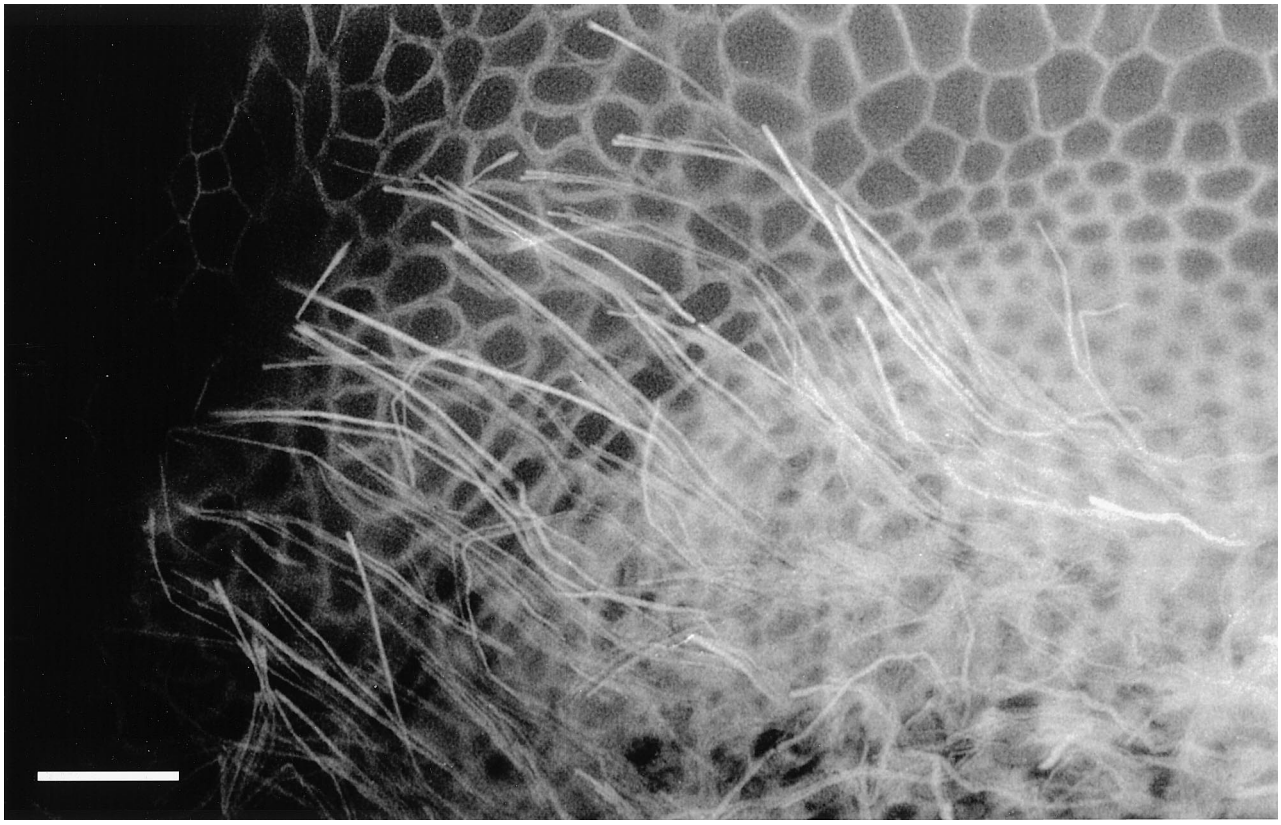

Fig. 6. Epifluorescent view of a whole mount of the crista ampullaris of a mature *pi/pi* mouse. Long and straight actin bundles extend from the sensory epithelium towards the basement membrane. The actin bundles progress in a course that is perpendicular to the plane of the luminal surface. Bar is 25 μm.

The primary reason why these mutant mice cannot hear is unclear. These mice seem to have a full complement of hair cells at the time of inner ear maturation. Moreover, we have measured the endocochlear potential (EP) in two 30-day old *pi/pi* mice. In each case, the EP was above 80 mV and thus not a likely source of the hearing loss (DFD, unpublished data). The presence of normal EP suggests that the profound hearing loss is most likely related to dysfunction in the inner hair cells or the afferent innervation.

The *sh2/sh2* mice showed no ABR responses to acoustic stimulation at any age. Some of the young *pi/pi* mice, however, did show ABR responses at 8 kHz, but only for stimuli above 90 dB SPL. Their limited response to 8 kHz temporally coincided with the presence of cytocauds in the organ of Corti, suggesting that cytocauds and (residual) hearing are not mutually exclusive.

It is not clear why hair cells should spend the energy and protein resources to form and/or maintain a cytocaud. Understanding the function of the mutated proteins will be of help in elucidating the reason for the presence of cytocauds. However, at present, the identity of the *pi* gene is unknown and the *sh2* gene, *Myo15* (Probst *et al*., 1998), has not yet been characterized with respect to its function.

There are several possible explanations for the presence of cytocauds. The first assumes that as a direct result of the mutation, cells are unable to correctly organize a subset of actin bundles. An alternative scenario is that hair cells extend cytocauds purposefully. It is possible that the cell has a specific need to extend a process, and the actin bundle serves as the mechanical force to maintain the projection. For instance, if inner hair cells are lacking a developmental cue from the basement membrane or the matrix, they might search for it by sending a process towards the matrix. If this scenario is correct, one implication is that the mutation primarily affects a non-hair cell structure, and the response of the hair cell is secondary. A third possibility for the presence of the cytocaud is that the inner hair cells and the vestibular hair cells in the *sh2* and *pi* mice maintain their connection with the basement membrane, and never detach from it during development. At the otocyst stage, all epithelial cells normally have contact with the basement membrane. Later, during normal ear development, the epithelium becomes pseudostratified, with hair cells detaching from the basement membrane. This takes place around developmental day E15 in normal mice. The actin bundle of the cytocaud is a scaffold that supports the extension to the basement membrane.

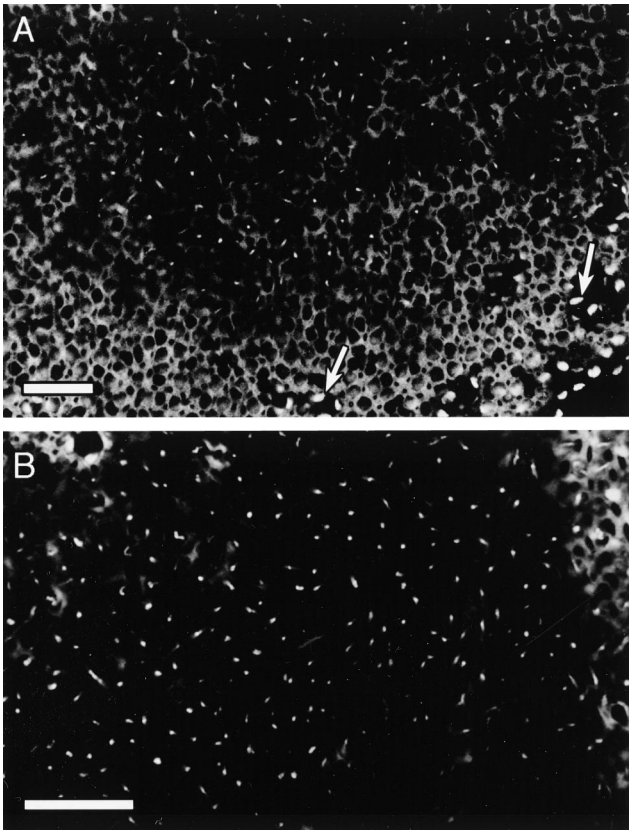

Fig. 7. CFM sections of *pi/pi* mice utricular whole mounts stained with phalloidin. (A) At a focal plane near the luminal surface, some hair cells demonstrate a faint actin-specific fluorescence in their cuticular plate. Hair cell stereocilia bundles are short (arrows). Some of the hair cells are (optically) sectioned beneath the cuticular plate. In these cells, one bright circle (or dot) is present at or near the center of the cell. B. At a lower focal plane, approximately 3 μm beneath the reticular lamina, confocal optical sections reveal the actin-positive dots. The diameter of the dots is relatively uniform among the cells throughout the utricle. Bar is 25 μm.

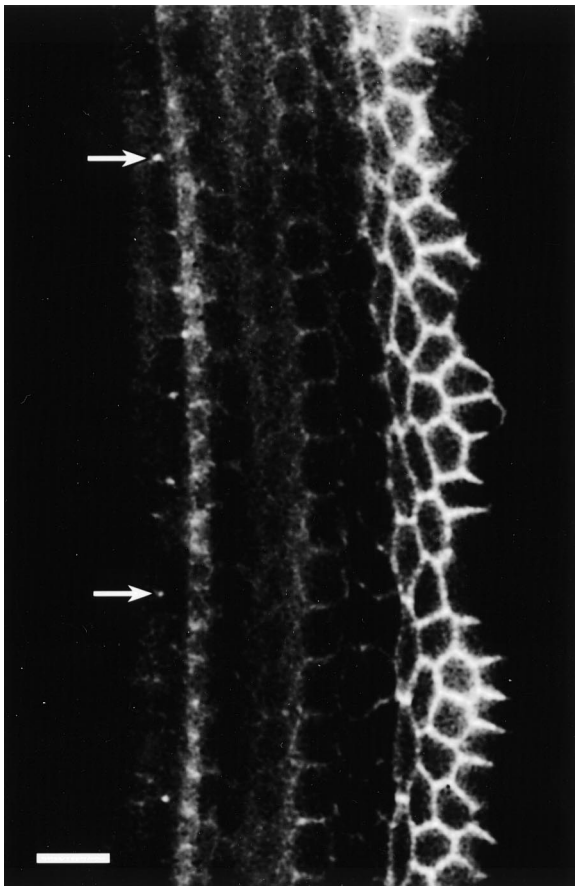

Fig. 8. An epifluorescent image from a whole mount of the basal turn of a 3-day old *pi/pi* mouse. The lateral aspect of the organ of Corti is on the right-hand side. Actin-positive dots (arrows) are observed in the inner hair cells at the focal plane immediately beneath the reticular lamina (luminal surface). Most of the cells display one bright dot. The intensity of the dots at this developmental stage is rather faint and variable among the different cells in the field of view. Bar is 10 μm.

It is important to integrate the morphological details with knowledge at the genetic level, in order to shed light on the raison d'être of the cytocaud and the role of the mutated gene products. Once the *pi* gene is known and the function of *Myo15* is better understood, integration of the morphology with the genetic data will be more informative. At present, the morphological data can provide some hints, which may be of help in understanding these mutations and the nature of the cytocaud. The distribution of the cytocaud is limited to the inner hair cell and type I vestibular hair cells. The main features that distinguish these cells from the other hair cells of the inner ear is the type of innervation. Cytocaud-containing cells are predominantly innervated by afferent neurons. Association between the pattern of innervation and the cytocaud is supported by the course of cytocaud extension in the vestibular versus auditory hair cells. In the vestibular epithelium, the cytocauds project in a straight basal course, directly

Fig. 9. TEM analysis of sectioned vestibular hair cells of mature *sh2* and *pi* mutant mice. The plane of sectioning is perpendicular to the reticular lamina. (A) The apical domain of a hair cell in the crista ampullaris (of the lateral semicircular canal) of a *pi/pi* mouse, with an actin bundle (white arrow) originating near the cuticular plate. A basal body (black arrow) is located distally from the actin bundle. Two dense regions that appear to contain cross-filaments are observed. (B) The nucleus (n) in the mid to lower domain of a vestibular *sh2/sh2* hair cell appears to flatten in the area of the actin bundle. Several small kinks are present in this area. (C) The basal domain of a utricular *sh2/sh2* hair cell (h) extends to the region of the supporting cells (s) and reaches the area of the basement membrane and the extracellular matrix (m) of the vestibular epithelium. (D) The actin bundle in one area of a *sh2/sh2* utricular hair cell is split into two different bundles, which appear to re-unite at a lower region (arrow). Bars are: 1 μm in (A); 2 μm in (B), (C) and (D).

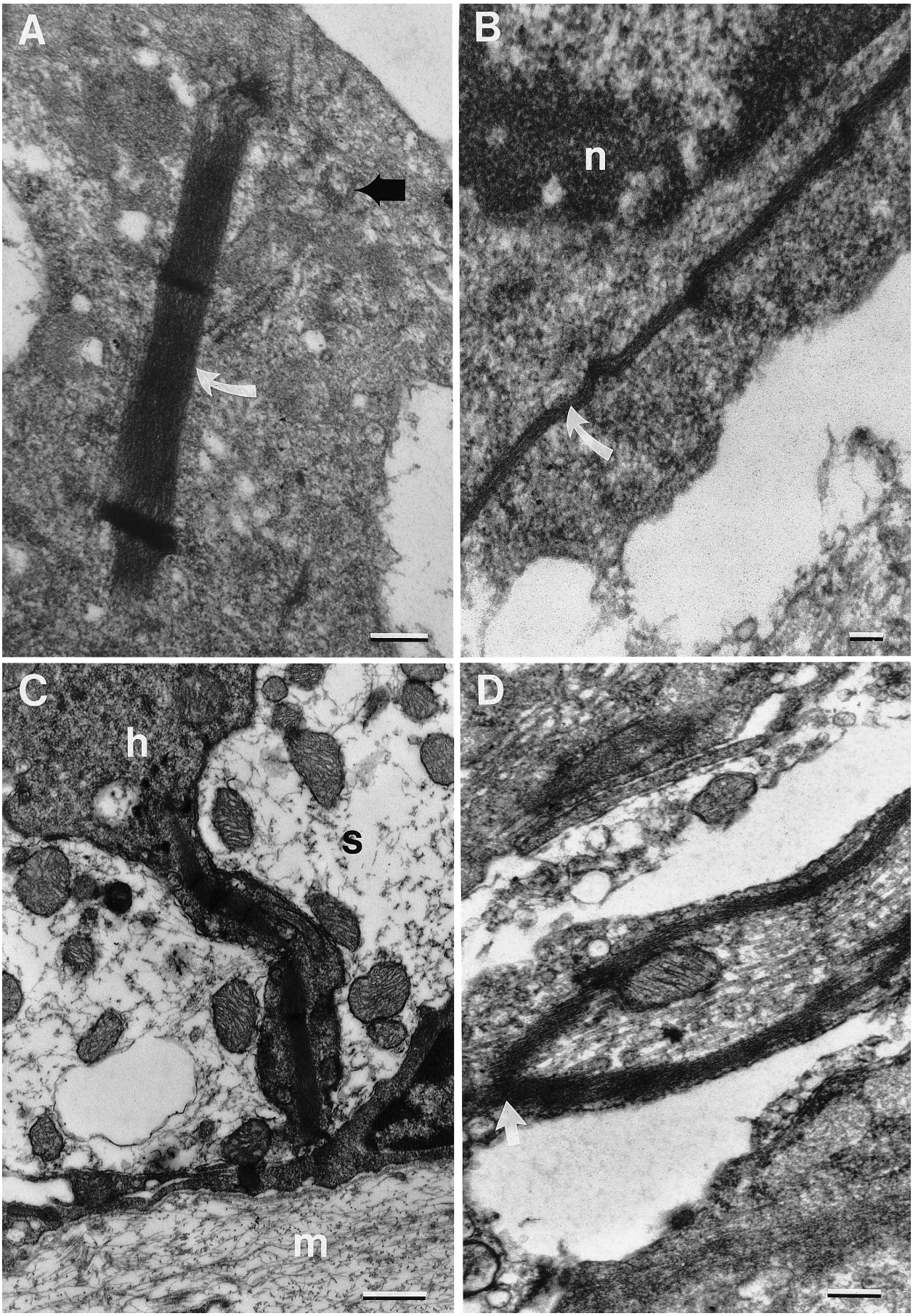
A
B
n
C
h
s
m
D

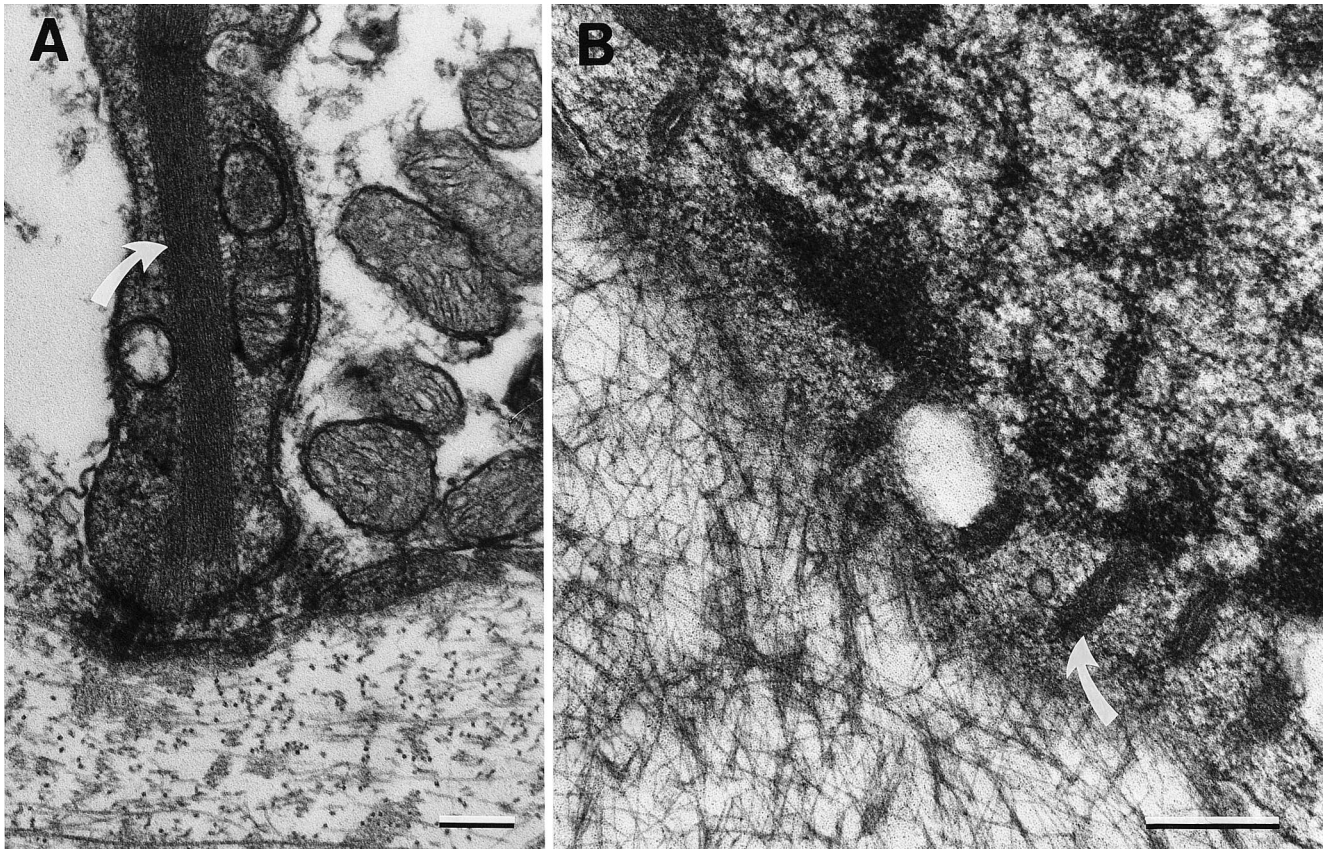

Fig. 10. TEM sections of the basal tips of cytocauds in vestibular hair cells in a *sh2/sh2* mouse. (A) The basal portion of the actin core is straight. The core bundle reaches the plasma membrane adjacent to the basement membrane. Cytoplasm and mitochondria surround the actin core of the cytocaud. Electron-dense material is found between the plasma membrane of the hair cell and the basal lamina. (B) The region of contact between the base (distal end) of the cytocaud and the extracellular material. Electron-dense finger-like protrusions (arrow) span the region between the hair cell and the matrix. The electron-dense protrusions measure 300 to 400 nm. The membrane of the hair cell and the basal lamina are less distinguishable in this area. Bars are: 1 μm in (A); 500 nm in (B).

towards the basement membrane beneath the hair cell, where afferent vestibular fibers reside. Cytocauds extending from inner hair cells travel in a medial direction, also in the direction of the afferent cochlear fibers. Based on the course of cytocaud projection and the innervation characteristics of the cytocaud-containing cells, we speculate that the inability to form a functional synapse or the absence of some molecular clues in the communication between the developing hair cell and neuron may constitute the primary problem in these mutations.

Mutation in a matrix protein (or a protein that mediates epithelial-matrix communication) may be an alternative explanation for extending a process towards the basement membrane, or for the failure to detach from the matrix. The contact between the basal tip of the cytocaud and the basement membrane is characterized by thin spike-like projections of unknown composition. The basal lamina may be discontinued at the site of contact. Finally, it is possible that the mutation in *Myo15* impairs its ability to physically pull the hair cell from the basement membrane. Further characterization of the molecular components in the contact area may shed light on the primary influence of the mutations and the reason for the presence of cytocaud.

In conclusion, we have demonstrated that inner hair cells and vestibular type I hair cells in two deaf and circling mutants, *sh2* and *pi*, produce cellular extensions towards the basement membrane. Direct contact with the basement membrane was confirmed for the vestibular cells. We named the entire cellular extension that reaches the basement membrane the cytocaud. Future research is needed to determine why hair cells keep this connection to the matrix, and how this is related to the mutation in *Myo15* and the *pi* genes.

Acknowledgments

We thank Gary Dootz for technical help, Karen Kobayashi, Nadine Brown and Graham Atkin for proofreading the manuscript, Joe Hawkins for helping in coining the name “cytocaud”, Donna Martin

for valuable discussions and Jill Karolyi for maintaining the mouse colony in the Dept. of Human Genetics. FJP was supported by a University of Michigan Rackham Graduate Fellowship. This work was supported by NIH NIDCD grants R01 DC01634 (YR), DC02982 (DK and DD), DC03049 (DK), DC00078 (DD and YR), NIH NICHD grant R01 30428 (SAC), and grants from the National Organization for Hearing Research and the Deafness Research Foundation (DK).

References

ANNIKO, M., SOBIN, A. & WERSALL, J. (1980). Vestibular hair cell pathology in the Shaker 2 mouse. *Archives of Oto-Rhino-Laryngology* **226**, 45–50.

AVRAHAM, K. B., HASSON, T., SOBE, T., BALSARA, B., TESTA, J. R., SKVORAK, A. B., MORTON, C. C., COPELAND, N. G. & JENKINS, N. A. (1997). Characterization of unconventional MYO6, the human homologue of the gene responsible for deafness in Snell's waltzer mice. *Human Molecular Genetics* **6**, 1225–1231.

BOCK, G. R. & STEEL, K. P. (1983). Inner ear pathology in the deafness mutant mouse. *Acta Oto-Laryngologica* **96**, 39–47.

ERNSTSON, S., LUNDQUIST, P. G., WEDENBERG, E. & WERSALL, J. (1969). Morphologic changes in vestibular hair cells in a strain of the waltzing guinea pig. *Acta Oto-Laryngologica* **67**, 521–534.

HASSON, T., GILLESPIE, P. G., GARCIA, J. A., MACDONALD, R. B., ZHAO, Y., YEE, A. G., MOOSEKER, M. S. & COREY, D. P. (1997). Unconventional myosins in inner-ear sensory epithelia. *Journal of Cell Biology* **137**, 1287–1307.

LIM, D. J. & ANNIKO, M. (1985). Developmental morphology of the mouse inner ear. A scanning electron microscopic observation. *Acta Oto-Laryngologica* - Supplement **422**, 1–69.

PROBST, F. J., FRIDELL, R. A., RAPHAEL, Y., SAUNDERS, T. L., WANG, A., LIANG, Y., MORELL, R. J., TOUCHMAN, J. W., LYONS, R. H., NOBEN-TRAUTH, K., FRIEDMAN, T. B. & CAMPER, S. A. (1998). Correction of deafness in shaker 2 mice by an unconventional myosin in a BAC transgene. *Science* **280**, 1444–1447.

RAPHAEL, Y., LENOIR, M., WROBLEWSKI, R. & PUJOL, R. (1991). The sensory epithelium and its innervation in the mole rat cochlea. *Journal of Comparative Neurology* **314**, 367–382.

SHER, A. E. (1971). The embryonic and postnatal development of the inner ear of the mouse. *Acta Oto-Laryngologica* —Supplement **285**, 1–77.

SLEPECKY, N. B. (1996). Structure of the mammalian cochlea. In *The Cochlea* (edited by DALLOS, P., POPPER, A. N. & FAY, R. R.) pp. 44–129. New York: Springer-Verlag.

SOBIN, A., ANNIKO, M. & FLOCK, A. (1982). Rods of actin filaments in type I hair cells of the Shaker 2 mouse. *Archives of Oto-Rhino-Laryngology* **236**, 1–6.

SOBIN, A. & FLOCK, A. (1981). Sensory hairs and filaments rods in vestibular hair cells of the waltzing guinea pig. Organization and identification of actin. *Acta Oto-Laryngologica* **91**, 247–254.

SOBIN, A. & FLOCK, A. (1983). Immunohistochemical identification and localization of actin and fimbrin in vestibular hair cells in the normal guinea pig and in a strain of the waltzing guinea pig. *Acta Oto-Laryngologica* **96**, 407–412.

STEEL, K. P. (1995). Inherited hearing defects in mice. *Annual Review of Genetics* **29**, 675–701.

STEEL, K. P. & BOCK, G. R. (1983). Hereditary inner-ear abnormalities in animals. Relationships with human abnormalities. *Archives of Otolaryngology* **109**, 22–29.

STEEL, K. P. & BROWN, S. D. (1996). Genetics of deafness. *Current Opinion in Neurobiology* **6**, 520–525.